Applied Catalysis B: Environmental 330 (2023) 122663

Contents lists available at ScienceDirect

Applied Catalysis B: Environmental

journal homepage: www.elsevier.com/locate/apcatb

Regulating the surface Au sites of Au/TiO_2 catalyst for achieving co-oxidation of HCHO and CO at room temperature

Xiaoxiao Qin [a,b], Min Chen [a,*], Xueyan Chen [a], Jianghao Zhang [a], Xiaoxin Wang [a], Jinhou Fang [c], Hong He [a,b], Changbin Zhang [a,b,c,**]

[a] State Key Joint Laboratory of Environment Simulation and Pollution Control, Research Center for Eco-Environmental Sciences, Chinese Academy of Sciences, Beijing 100085, China
[b] University of Chinese Academy of Sciences, Beijing 100049, China
[c] Weifang Research Institute of Materials and Technology for Eco-Environmental Protection, Weifang, Shandong, 261300, China

ARTICLE INFO

Keywords:
Au/TiO_2
Active sites
Surface Au sites
HCHO
CO

ABSTRACT

While supported Au catalyst is active for formaldehyde (HCHO) or CO oxidation alone at room temperature, it has not been reported hitherto to efficiently catalyze co-oxidation of HCHO and CO. In this work, we prepared the fresh Au/TiO_2 (Au/Ti-F) and the Au/Ti-O by pretreating Au/Ti-F at 300 °C under O_2 atmosphere. The Au/Ti-F is only active for HCHO oxidation during HCHO and CO co-oxidation, while the Au/Ti-O shows high efficiency for both HCHO and CO oxidation, achieving 100 % conversions at room temperature. Detailed characterization and DFT calculation indicate that only the Au-Ti interface sites were exposed on Au/Ti-F because other Au sites on Au NPs were covered by $Au(OH)_n$ ($0 < n < 3$). Over Au/Ti-O, besides the active sites at the Au-Ti interface, the metallic Au sites away from the interface were formed during the high-temperature treatment. HCHO oxidation occurs at the Au-Ti interface sites while CO oxidation occurs at the metallic top Au sites; hence high activity for HCHO and CO co-oxidation was achieved over Au/Ti-O. The obtained insight into the dual Au sites will benefit future design of supported Au catalysts.

1. Introduction

Formaldehyde (HCHO) and carbon monoxide (CO) are both indoor air pollutants. HCHO is usually sourced from various building and decorative materials [1], while CO comes from incomplete combustion during cooking and supply heating [2]. These two pollutants often coexist in some special spaces, such as kitchen, submarines and manned spacecraft [3]. Since long-term exposure to HCHO and CO is harmful to human health, it is imperative to develop efficient methods and materials to catalyze the co-oxidation of indoor air HCHO and CO.

Catalytic oxidation is a promising method for indoor air purification [4,5]. In particular, the supported noble metal (Pt [6,7], Pd [8,9], and Au [10,11]) catalysts have attracted extensive attention in recent years due to their high efficiency that can decompose HCHO or CO into harmless CO_2 at ambient temperature. Pt-based catalysts have shown excellent performance for HCHO oxidation at room temperature even at a high space velocity. However, the catalytic activity for CO oxidation is inhibited by the CO self-poisoning effect over Pt catalysts at low temperature [12,13]. Pd-based catalysts also exhibit promising performance for HCHO oxidation at room temperature but show a much lower activity on the oxidation of CO [14]. Although the catalytic activity of CO oxidation over Pt and Pd catalysts can be improved by increasing the reaction temperature, the temperature of complete conversion (approximately 150 °C) is too high for wide application [15,16]. It is worth noting that supported Au catalysts have shown outstanding catalytic performance for both HCHO and CO oxidation alone at room temperature [10,17], indicating that the Au catalyst is the most promising catalyst to achieve the co-oxidation of HCHO and CO. However, there is no related reports on the elimination of coexisting HCHO and CO to date.

Au/TiO_2 catalysts have attracted vast interests since Haruta et al. discovered the excellent activity of supported Au nanoparticles (NPs) for various oxidation reactions [10,18,19]. The prevailing view of CO oxidation on Au/TiO_2 catalysts is that the Au-Ti interface is regarded as

* Corresponding author.
** Corresponding author at: State Key Joint Laboratory of Environment Simulation and Pollution Control, Research Center for Eco-Environmental Sciences, Chinese Academy of Sciences, Beijing 100085, China.
E-mail addresses: minchen@rcees.ac.cn (M. Chen), cbzhang@rcees.ac.cn (C. Zhang).

https://doi.org/10.1016/j.apcatb.2023.122663
Received 12 January 2023; Received in revised form 16 March 2023; Accepted 17 March 2023
Available online 20 March 2023

the active site [20–26]. Meanwhile, previous studies have indicated that HCHO is mainly adsorbed on TiO_2 and the HCHO oxidation reaction is confined to the metal-TiO_2 interface [6,7,27,28]. Then, it arises question about whether the competition of active site between HCHO and CO will lead to the preferential oxidation of HCHO or CO? It is reported that top Au sites play the critical role on Au/Al_2O_3, or Au supported on other irreducible supports [29–32]. Obviously, the role of the top Au sites on Au/TiO_2 seems to be neglected. It brings another question: if there are double active sites on Au/TiO_2 catalyst, can the oxidation of HCHO and CO not interfere with each other?

On this basis, we prepared the fresh Au/TiO_2 (Au/Ti-F) and the Au/Ti-O by pretreating Au/Ti-F at 300 °C under O_2 atmosphere. We observed that only the Au-Ti interface sites were exposed on Au/Ti-F because the top Au sites on Au NPs were covered by $Au(OH)_n$ ($0 < n < 3$). While on Au/Ti-O catalyst, apart from the active sites at the Au-Ti interface, the metallic top Au sites away from the interface were formed during the high-temperature treatment. When HCHO and CO co-exist during reaction, the CO oxidation can occur on top Au sites while the Au-Ti interface sites are occupied by HCHO oxidation; thus, the Au/Ti-O catalyst is able to efficiently achieve the co-oxidation of HCHO and CO under ambient conditions.

2. Experimental section

2.1. Synthesis of Au/TiO_2 catalysts

The Au/TiO_2 catalysts were prepared by a deposition-precipitation method at room temperature with a mass loading of 1.3 wt. % (ICP-OES results). Typically, $HAuCl_4{\cdot}3\,H_2O$ (Sigma-Aldrich, 99.9 %) was first dissolved in deionized water, followed by adjusting the pH to ~9.0 with 0.25 mol/L NaOH solution before adding TiO_2 (P25, Degussa). After that the pH of mixture was adjusted with 0.25 mol/L NaOH solution until the pH stabilized at 8.6–9.0. The solution was stirred vigorously using a magnetic stirrer during the above procedures. The precipitate was thoroughly washed with deionized water to remove any possible ionic residues, and the solid obtained was dried at 50 °C in air overnight. The as-prepared sample was named Au/Ti-F, while the sample was named Au/Ti-O after pretreating Au/Ti-F with 10 % O_2/N_2 for 2 h at 300 °C.

2.2. Catalyst characterization

The actual loadings of Au were determined using inductively coupled plasma optical emission spectrometer (ICP-OES) on Agilent ICPOES730 under 1000 W radiofrequency power. 0.05 g sample was digested with aqua regia and hydrofluoric acid at 150 °C. High-angle annular dark-field scanning transmission electron microscopy (HAADF-STEM) was performed on a JEOL JEM-ARM 200F microscope with a Cs-corrected probe operated at 200 kV, and high-resolution transmission electron microscopy (HRTEM) images were obtained on a JEM 2100 PLUS microscope with 200 kV acceleration voltage. Typically, a drop of the nanoparticle solution was dispensed onto a 3 mm carbon-coated copper grid. Excess solution was removed using an absorbent paper, and the sample was dried at 50 °C overnight.

X-ray photoelectron spectroscopy (XPS) measurements were performed using an ESCALAB250Xi system, equipped with an X-ray anode operated at 225 W and 15 kV (Al K_α radiation, $h\nu = 1486.6$ eV). The C 1 s peak (284.8 eV) was used to calibrate the binding energy values. H_2-temperature programmed reduction (H_2-TPR) and temperature programmed desorption (TPD) were carried out on a Chemisorption Analyzer (Micromeritics AutoChem 2920) equipped with a mass spectrometer. For H_2-TPR experiments, a 0.05 g sample was pre-treated with 10 % O_2/He for 20 min at 50 °C or 300 °C for Au/Ti-F and Au/Ti-O, respectively. The temperature was increased from −20 to 500 °C at a rate of 10 °C/min, and the H_2 consumption was monitored using TCD after the removal of produced H_2O. For TPD testing, a 0.05 g sample was purged by UHP Ar (30 mL/min) for 30 min at room temperature, and then the temperature was ramped to 300 °C (15 °C/min). The TPD profiles were obtained using a TCD detector and mass spectrometer.

In situ diffuse reflectance infrared Fourier transform spectroscopy (in situ DRIFTS) experiments were performed with a Thermo Fisher iS 50 Spectrometer coupled with a Praying Mantis Diffuse Reflection Accessory from Harrick. The flow of the feed gas mixture was controlled using mass flow meters. In each test, the sample was purged with N_2 (50 mL/min) for 1 h before recording the background. All spectra were measured with a resolution of 4 cm^{-1} and accumulation of 32 scans.

2.3. Evaluation of catalytic performance

The activities of Au/TiO_2 samples for catalytic oxidation of HCHO and CO were determined in a fixed-bed quartz flow reactor at 25 °C with a gas mixture containing 300 ppm HCHO or/and CO, 20 % O_2, 35 % relative humidity (RH) and N_2 balance at a total flow rate of 30 mL/min with a gas hourly space velocity (GHSV) of 60,000 mL $(g_{cat}{\cdot}h)^{-1}$ or 200,000 mL$(g_{cat}{\cdot}h)^{-1}$. While CO was directly obtained by dilution of compressed CO, gaseous HCHO was obtained by flowing N_2 through a paraformaldehyde container in a water bath, and the concentration of inlet HCHO was controlled by adjusting the temperature of the water bath. Water vapor was generated by flowing N_2 through a water bubbler at 25 °C, and the relative humidity in the reaction atmosphere was controlled by adjusting the flow rate of the N_2 purge gas and measured by a hygrometer. The inlet and outlet gases were monitored with an infrared spectrometer equipped with a gas cell and a deuterated triglycine sulfate (DTGS) detector. The peaks at 2898.57–2895.07 cm^{-1} and 2198.14–2194.94 cm^{-1} were used to determine the concentration of HCHO and CO, respectively.

The activation energy (E_a) of CO oxidation at Au-Ti interface was tested over the Au/Ti-F sample with a gas mixture containing 300 ppm CO, 20 % O_2, 35 % RH and N_2 balance. While the E_a of CO oxidation at top Au sites was tested over the Au/Ti-O sample with a gas mixture containing 300 ppm CO, 300 ppm HCHO, 20 % O_2, 35 % RH and N_2 balance. The conversion of CO was controlled below 15 %, and the E_a was calculated from the CO conversion rate at each test temperature.

2.4. DFT calculation

Calculations on the interaction of Au (111) with O_2 were performed with the code VASP. The Perdew-Burke-Ernzerhof (PBE) GGA exchange-correlation functional was applied. A periodic slab with 2×2 surface unit cells was used to model the Au (111) surface. The model contained 36 atoms for Au (111). The bottom two layers of Au were fixed in the process of structure optimization. The vacuum gap thickness was 15 Å. Gamma-centered k-point meshes of $2 \times 2 \times 1$ were employed. Structures were relaxed until the forces acting on each atom were smaller than 0.02 eV/Å.

3. Results and discussion

3.1. Catalytic performance of Au/TiO_2 catalysts

The as-prepared Au/TiO_2 catalysts all presented a mass loading of about 1.3 wt. % (ICP results, as shown in Table S1). The Au/Ti-F and Au/Ti-O catalysts were first evaluated for HCHO and CO co-oxidation at room temperature. Fig. S1 shows the HCHO and CO conversion levels with time-on-stream in HCHO and CO co-oxidation, and Fig. 1a presents the HCHO and CO conversion after HCHO and CO co-oxidation for 5 h for better comparison. The Au/Ti-F catalyst exhibited high activity for HCHO destruction, while it showed no activity for CO oxidation, presenting 100 % HCHO conversion and only around 2.3 % CO conversion after 5 h. In contrast, the Au/Ti-O catalyst demonstrated high activity for simultaneous HCHO and CO oxidation, maintaining complete conversion of both HCHO and CO to CO_2 during the 5 h reaction. The CO oxidation level in the absence of HCHO was also measured over the Au/

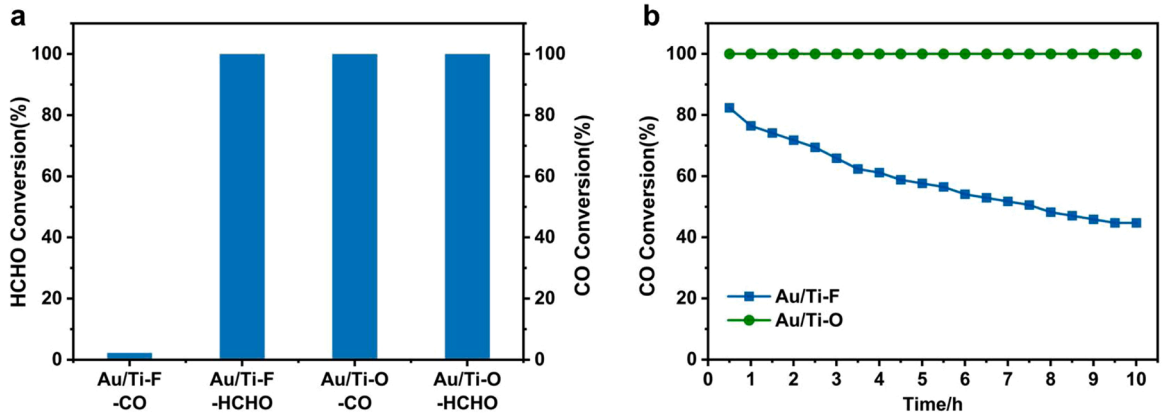

Fig. 1. Catalytic performance of Au/TiO_2 catalysts at room temperature: (a) HCHO and CO conversion after HCHO and CO co-oxidation for 5 h, (b) CO conversion with time-on-stream in CO oxidation alone. Reaction conditions: (a) 300 ppm HCHO, 300 ppm CO, 20 % O_2, 35 % RH, GHSV= 60,000 mL $(g_{cat}\cdot h)^{-1}$; (b) 300 ppm CO, 20 % O_2, 35 % RH, GHSV= 60,000 mL $(g_{cat}\cdot h)^{-1}$.

Ti-F and Au/Ti-O catalysts. As shown in Fig. 1b, Au/Ti-F exhibited some activity, with 45 % CO conversion after 10 h of reaction at room temperature, while Au/Ti-O presented much higher performance for CO oxidation than Au/Ti-F, maintaining complete CO conversion for 10 h.

These results show that the presence of CO had no significant effect on the HCHO oxidation performance of both the Au/Ti-F and Au/Ti-O catalysts, while the presence of HCHO significantly limited the CO oxidation activity of the Au/Ti-F catalyst. Note that the O_2 pretreatment at 300 °C had no influence on HCHO oxidation, but significantly promoted the performance for CO oxidation over Au/Ti-O. The interface sites on Au/TiO_2 are always considered to be active sites for CO oxidation [20,33–37]. Hence, we propose that there are two possible reasons for the significantly different CO oxidation performance in HCHO and CO co-oxidation on Au/Ti-F and Au/Ti-O catalysts related to the active sites. The first reason is that the interface sites of Au/Ti-F and Au/Ti-O might be different and these sites on Au/Ti-O were more active than those of Au/Ti-F. The second is that the interface sites on Au/Ti-O and Au/Ti-F were similar to each other, and new active sites might be created on the Au/Ti-O catalyst during the O_2 pretreatment at 300 °C.

Previous studies [6,7,27,28] have shown that HCHO is mainly adsorbed on TiO_2, which could be also confirmed here by the in situ DRIFTS results of HCHO adsorption on TiO_2 and Au/TiO_2 catalysts (Fig. 2a). The spectrum shows that HCHO was adsorbed on TiO_2 in the form of dioxymethylene (DOM). After introducing Au, the DOM is converted to formate (HCOO) on the Au/TiO_2 catalysts as it reacts with surface active oxygen species and OH groups activated by Au sites. Hence, HCHO is adsorbed on TiO_2 sites in the form of formate on Au/TiO_2, and the HCHO oxidation reaction can only occur at the Au-Ti interface. The interface activity of the two catalysts was determined by comparing their catalytic oxidation performance for HCHO, shown in Fig. 2b and Fig. S2. The Au/Ti-F and Au/Ti-O catalysts exhibited similar HCHO catalytic performance for HCHO oxidation alone with or without water vapor in the gas mixture (Fig. S2), and even with a high GHSV of 200,000 mL $(g_{cat}\cdot h)^{-1}$ (Fig. 2b). The dynamic in situ DRIFTS results in Fig. S3 indicate that the intensities of formate peaks on both Au/Ti-F and Au/Ti-O sharply dropped after O_2 purging for 30 min and then completely disappeared after exposure to a flow of O_2 +H_2O+N_2 for 30 min, also revealing the similar catalytic performance of Au/Ti-F and Au/Ti-O. The similar HCHO catalytic performance of Au/Ti-F and Au/Ti-O for ambient HCHO oxidation indicates that the structures at the Au-Ti interface were similar. Therefore, we can prove that the interfacial activities of the two catalysts are similar to each other, excluding the influence of interface sites on CO oxidation.

3.2. *Physical structure of Au nanoparticles*

The particle size and dispersion of Au species were explored through high-angle annular dark-field scanning transmission electron microscopy (HAADF-STEM). As shown in Fig. 3, Fig. S4 and S5, the Au NPs were spherical and Au (111) facets and Au (200) facets were observed on

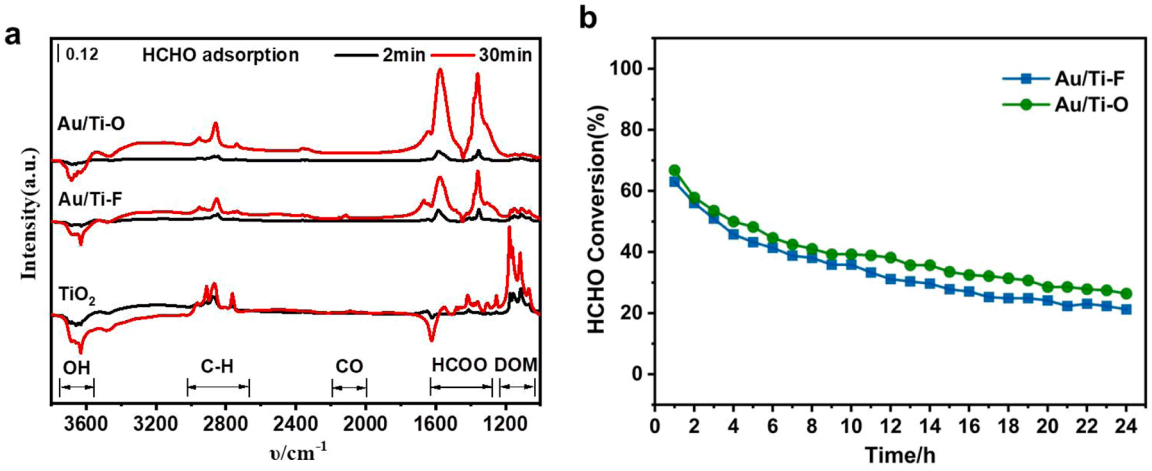

Fig. 2. a, in situ DRIFTS study of HCHO adsorption on catalysts; b, HCHO conversion with time-on-stream in HCHO oxidation alone, reaction conditions: 300 ppm HCHO, 20 % O_2, 35 % RH, GHSV= 200,000 mL $(g_{cat}\cdot h)^{-1}$.

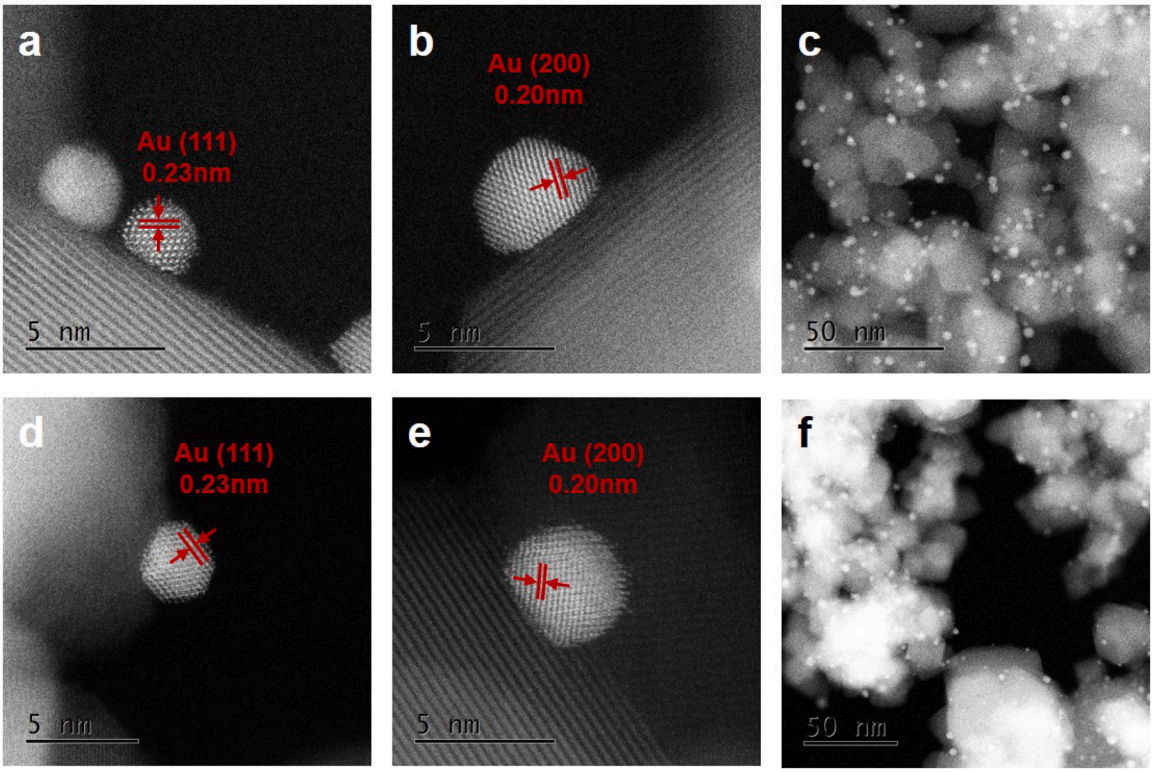

Fig. 3. HAADF-STEM images (dark field) of Au/Ti-F (a-c) and Au/Ti-O (d-f).

both Au/Ti-F and Au/Ti-O catalysts [20,21]. The mean particle sizes were determined by a statistical analysis of 200 particles, showing that Au was highly dispersed as particles of about 3.2 nm and 3.0 nm in diameter on the Au/Ti-F and Au/Ti-O catalysts, respectively (Table S1). It has been revealed that supported Au NPs with a particle size of about 3 nm are most effective for CO oxidation [38,39]. Thus, the prepared Au/TiO_2 catalysts with similar particle size are suitable for investigating the active sites and mechanism on supported Au catalysts. Kuwauchi et al. [40] have reported that Au NPs could be occasionally encapsulated in O_2 (100 Pa) treatment, and a partial encapsulation of Pd clusters with TiO_2 could be also induced by high temperature reduction in our previous study [9]. We did not observe the encapsulation of Au species on the Au/Ti-O catalyst, indicating that O_2 pretreatment at 300 °C has limited influence on the particle size and intrinsic structure of Au NPs and the Au-Ti interface.

3.3. Chemical state of Au species

The catalysts were next characterized by XPS and the results are shown in Fig. 4. The Au $4f_{7/2}$ peak was employed to analyze the chemical state of surface Au species. Two peaks at 83.5 eV and 84.2 eV were observed over the Au/TiO_2 catalysts and attributed to Au^0 and Au^+ species, respectively [41,42]. The distribution of Au^0 and Au^+ species was calculated and shown in Table S1. The contents of metallic Au species were 19 % and 80 % on Au/Ti-F and Au/Ti-O, respectively, indicating that surface Au species were mainly in oxidized and metallic states on the Au/Ti-F and Au/Ti-O catalysts, respectively. Moreau et al. [43] reported a systematic study of the effect of pH on the kinds of Au species during the preparation of Au/TiO_2 catalysts. At pH 8 and above, the $Au(OH)_4^-$ anion is the dominant species in solution, and the adsorbed species is $Au(OH)_3$ on TiO_2 surface. We adjusted the pH to 8.6–9.0

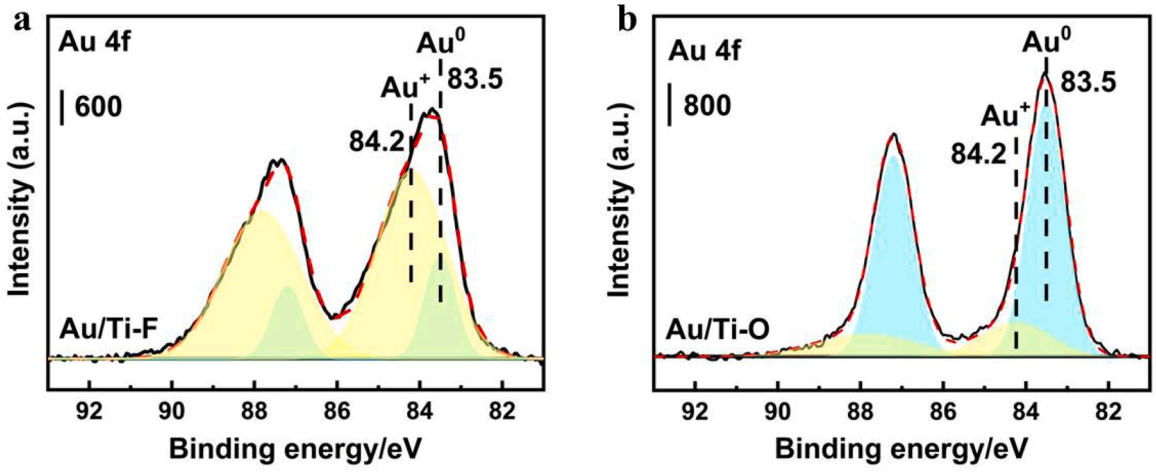

Fig. 4. Au 4f XPS spectra of Au/Ti-F (a) and Au/Ti-O (b).

during the preparation of Au/TiO_2 catalysts, and the XPS results suggest the oxidized state of surface Au species on Au/Ti-F, hence, we believe that Au species were deposited on TiO_2 mainly as $Au(OH)_n$ ($0 < n < 3$) in this work. Temperature programmed desorption (TPD) was performed to further confirm the kinds of surface Au species. Fig. S6 shows that compared with Au/Ti-O, Au/Ti-F exhibited a H_2O desorption peak at 250–400 °C, which is assigned to the decomposition of $Au(OH)_n$ [44], also indicating that the surface Au species was $Au(OH)_n$ on Au/Ti-F. Combining these findings with the HAADF-STEM results and considering the limited testing depth of XPS, we believe that the surface Au species was $Au(OH)_n$, covering the intrinsic Au NPs in the metallic state on Au/Ti-F. The surface $Au(OH)_n$ species were decomposed to metallic Au species during O_2 pretreatment at 300 °C on Au/Ti-O, resulting in the enhancement of the metallic Au percentage. These results suggest that surface Au species were in much different states on Au/Ti-F and Au/Ti-O; the Au species were mainly coordinated and covered with OH^- groups on Au/Ti-F, while mainly exposed as metallic Au sites on Au/Ti-O.

The XPS spectra of Ti 2p and O 1s over TiO_2, Au/Ti-F and Au/Ti-O were shown in Fig. S7. The peaks at 458.8 and 464.5 eV were attributed to Ti^{4+} of TiO_2 support for all the samples, and no peak of Ti^{3+} (~456 eV) was observed on TiO_2, Au/Ti-F and Au/Ti-O [45], indicating that Au species and O_2 pretreatment did not induce oxygen vacancies on TiO_2 (Fig. S7a). The O 1s spectra of the samples (Fig. S7b) were analyzed in terms of two component deconvolution. The major component O_I at 530.0 eV was related to lattice oxygen, while minor component O_{II} at 531.7 eV was attributed to surface oxygen [46]. As shown in Table S1, the concentrations of O_{II} were all about 15 % on TiO_2, Au/Ti-F and Au/Ti-O, indicating the same chemical state of TiO_2 support for all the samples. The XPS results of Ti 2p and O 1s reveal that O_2 pretreatment at 300 °C had limited influence on TiO_2 support.

Since the vibrational mode of adsorbed CO can be correlated with the electronic charge of Au species [39,47], in situ DRIFTS of CO adsorption was next measured to further investigate the structure of Au NPs on Au/Ti-F and Au/Ti-O. The in situ DRIFTS spectra of CO adsorption at room temperature on Au/TiO_2 catalysts and TiO_2 reference sample are shown in Fig. 5. No CO peak was observed on pure TiO_2, revealing that CO was only adsorbed on Au sites at room temperature (Fig. 5a). The peak at 2154 cm^{-1} was ascribed to CO adsorption on $Au^{\eta+}$ ($1 < \eta \leq 3$) sites on Au/Ti-F catalyst [48]. A feature at 2110 cm^{-1} that appeared on the Au/Ti-F catalyst was due to CO adsorption on $Au^{\delta+}$ ($0 < \delta \leq 1$) [49,50]. The peak shifted to 2106 cm^{-1} after 30 min exposure on Au/Ti-F, which was attributed to the electron transfer from CO to Au, resulting in a red shift of the CO adsorption peak [48,50,51]. Only a feature at 2112 cm^{-1} was observed on the Au/Ti-O catalyst, which was assigned to CO adsorption on $Au^{\delta+}$ ($0 < \delta \leq 1$) [49,50]. Combining this data with the XPS results, the distinctly higher intensity of CO adsorption on Au/Ti-F was due to the presence of more Au species in an oxidized state on Au/Ti-F than on Au/Ti-O. The absence of a CO adsorption peak on metallic Au species is due to the weak adsorption of CO on Au^0 at room temperature, as well as possible overlap with the peak of CO adsorption on $Au^{\delta+}$ [50,52]. Fig. 5b and S8 show the dynamic changes of IR spectra during purging with N_2 for 5 min after CO adsorption. The rapid decrease in the intensities of CO adsorption peaks on Au/Ti-F and Au/Ti-O indicates that CO was weakly adsorbed on both Au/Ti-F and Au/Ti-O. Hence, the CO adsorption results reveal significant differences between Au/Ti-F and Au/Ti-O in the surface Au NPs states, which might result in distinct catalytic oxidation performance. The Au species were mainly in the oxidized state on Au/Ti-F with stronger adsorption capacity for CO, which might affect the activation of oxygen. By contrast, the surface of Au/Ti-O mainly consisted of metallic Au species with weak adsorption capacity for CO, exposing the active sites to activate oxygen.

The significant difference of Au NPs between Au/Ti-F and Au/Ti-O was further confirmed by H_2-temperature programmed reduction (H_2-TPR) and temperature programmed desorption (TPD). As shown in Fig. 6a, Au/Ti-F exhibited two reduction peaks at 20 °C and 332 °C, which were mainly ascribed to the reduction of surface oxygen species and $Au(OH)_n$ [44,53], respectively. However, the latter peak completely disappeared on Au/Ti-O after O_2 pretreatment at 300 °C, due to the decomposition of $Au(OH)_n$ during the pretreatment. Along with the XPS results, the H_2-TPR results also demonstrate that the status of Au species on these two Au/TiO_2 catalysts was significantly different. The Au sites on top of Au NPs on the Au/Ti-F sample are covered by $Au(OH)_n$, while no $Au(OH)_n$ species covered the NPs on Au/Ti-O. Furthermore, the higher intensity of the surface oxygen reduction peak at 20 °C on Au/Ti-O indicates the higher oxygen activation capacity of Au/Ti-O compared to Au/Ti-F. The TPD results (Fig. 6b-d) show that Au/Ti-O exhibited a pronounced H_2O desorption peak at 62 °C, which was assigned to the desorption of weakly adsorbed H_2O on the Au NPs. In contrast, there is no peak below 90 °C for Au/Ti-F, indicating that there are new adsorption sites on the surface of Au NPs over Au/Ti-O. The shoulder peak at higher temperature was attributed to the desorption of adsorbed H_2O on TiO_2 or at the interface. Saavedra et al. [54]. reported that weakly adsorbed H_2O on TiO_2 could facilitate O_2 activation at the interface. Similarly, weakly adsorbed H_2O on Au NPs could be also beneficial to O_2 activation over Au/Ti-O. The above results indicate that there are double active sites for O_2 activation on the Au/Ti-O catalyst, one at the Au-Ti interface and another on the top of Au NPs away from the interface.

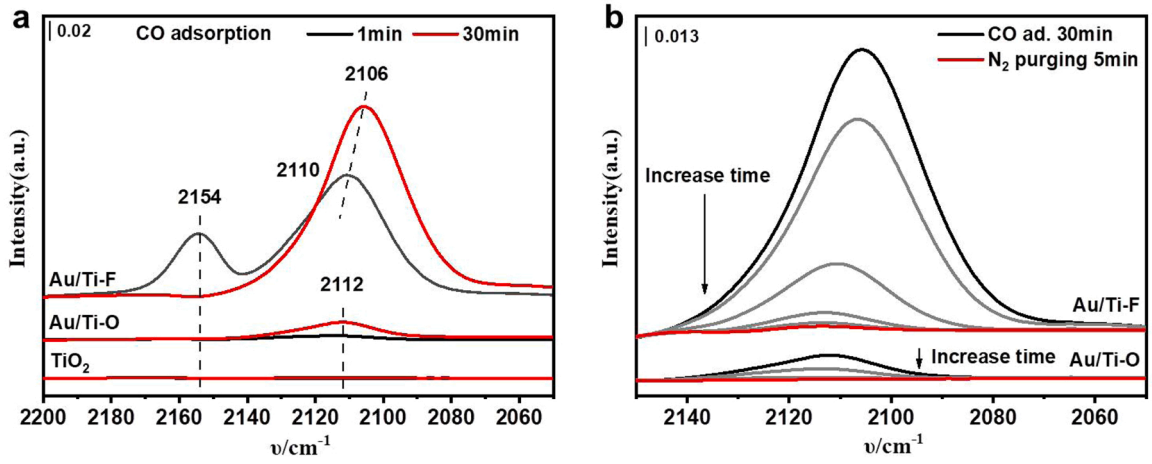

Fig. 5. a, in situ DRIFTS study of CO adsorption on catalysts; b, IR spectral development during N_2 purging for 5 min after CO adsorption (CO ad.) for 30 min over Au/Ti-O and Au/Ti-F.

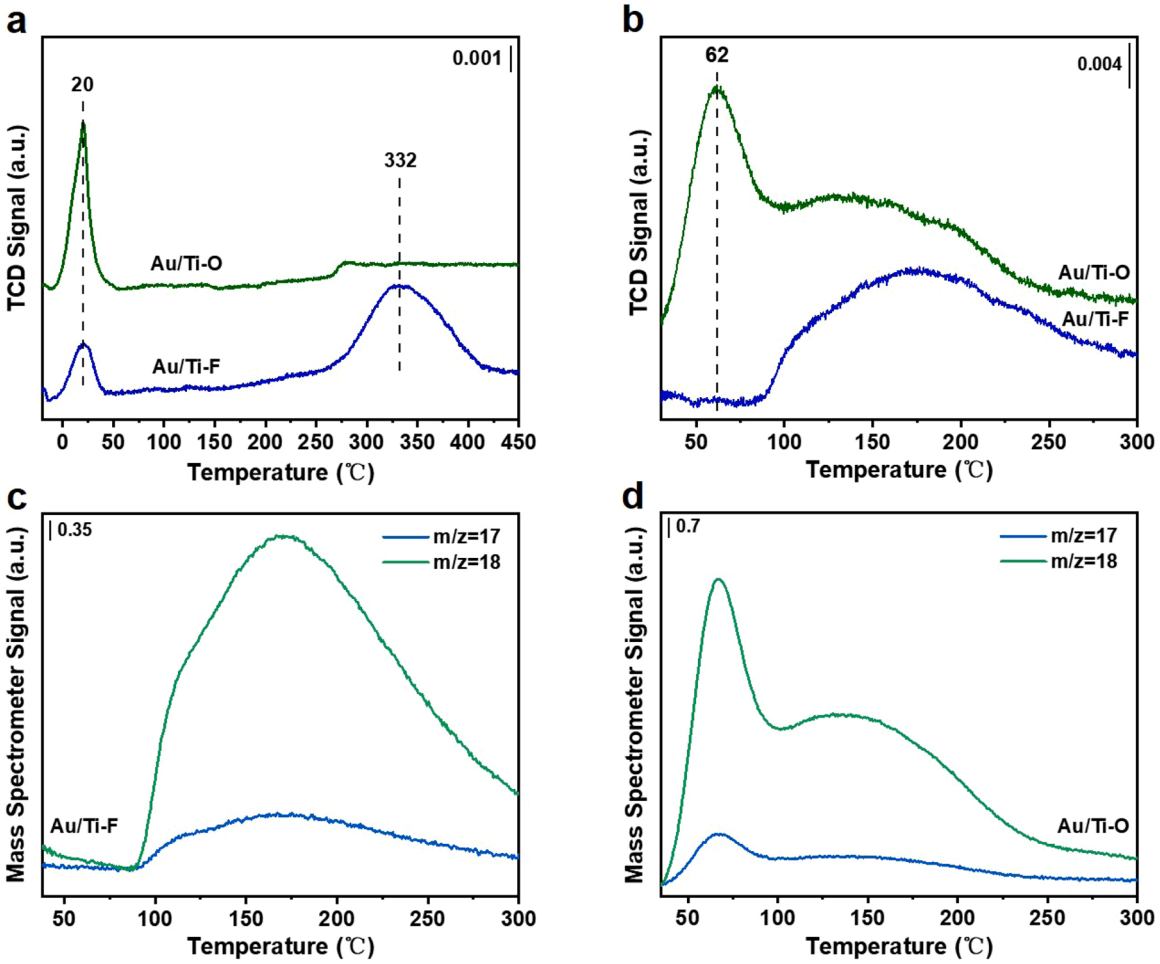

Fig. 6. H_2-TPR (a) and TPD (b-d) results for Au/Ti-F and Au/Ti-O. a-b, TCD signal; c-d, mass spectrometer signal.

3.4. Metallic top Au species as more active sites than interface Au sites

These findings indicate that top Au sites on Au NPs in the Au/Ti-F sample are covered by $Au(OH)_n$ ($0 < n < 3$), while the metallic Au species were dominant on the Au/Ti-O sample, and the activation capacity of Au/Ti-O was significantly higher than that of the Au/Ti-F catalyst. This suggests that the metallic top Au sites produced through the decomposition of $Au(OH)_n$ species under O_2 pretreatment at 300 °C should be also active sites alongside interface sites on Au/Ti-O catalyst. To further confirm this hypothesis, density functional theory (DFT) calculations were next performed to compare the O_2 activation on the Au sites and $Au(OH)_n$ sites. As shown in Fig. S9, the adsorption energy of O_2 on Au sites is −0.15 eV, which is stronger than that of O_2 on $Au(OH)_n$ sites (−0.08 eV). Besides, the bond length of O_2 is 1.30 Å after adsorption on Au sites while 1.25 Å after adsorption on $Au(OH)_n$ sites, indicating that O_2 is more easily activated on Au sites than $Au(OH)_n$ sites. To evaluate and compare the activity of Au-Ti interface sites and the top Au sites for CO oxidation, we further carried out kinetic measurements of CO oxidation alone over Au/Ti-F, and also HCHO and CO co-oxidation over Au/Ti-O, and then calculated the activation energy (E_a) of CO oxidation at Au-Ti interface sites and the top Au sites, respectively. As shown in Fig. S10 and Table S2, the E_a of CO oxidation are 30.0 kJ/mol and 16.6 kJ/mol over Au/Ti-F and Au/Ti-O, respectively, indicating the higher intrinsic activity of the top Au sites than Au-Ti interface sites. These results confirm that the presence of newly-formed top Au sites is responsible for the higher CO conversion on Au/Ti-O in HCHO and CO co-oxidation (Fig. 1a) than on Au/Ti-F for CO oxidation alone (Fig. 1b). Hence, based on all the experimental and DFT results, we concluded that the different activities of Au/Ti-F and Au/Ti-O catalysts for catalytic oxidation of HCHO and CO can be attributed to the double active sites on Au/Ti-O catalyst. In addition to the active sites at the Au-Ti interface, metallic Au sites on the catalyst surface are more active sites.

3.5. Reaction mechanisms on Au/TiO_2 catalysts

Based on the above results, possible reaction routes are illustrated in Fig. 7. O_2 activation (process 1) occurs at the Au-Ti interface for Au/Ti-F (Fig. 7a), and at the Au-Ti interface and also top Au sites on Au NPs away from the interface for Au/Ti-O (Fig. 7b). Considering that HCOO adsorbed on TiO_2 sites are delivered to the active interface sites and then react with active oxygen species to form CO_2 and H_2O (process 2), HCHO oxidation takes precedence over CO oxidation on the Au-Ti interface and directly leads to the inhibition of CO oxidation over Au/Ti-F in HCHO and CO co-oxidation. CO oxidation has two routes on Au/Ti-O at room temperature: route 1, CO diffuses to the interface and then reacts with active oxygen (process 3); route 2, CO reacts with active oxygen on top Au sites on Au NPs away from the interface (process 4). When there is no HCHO in the flow, CO oxidation can occur through route 1 over Au/Ti-F and through both route 1 and 2 on Au/Ti-O. However, when HCHO is present, route 1 does not occur on Au/Ti-F since HCHO oxidation takes precedence over CO oxidation at the Au-Ti interface, while CO oxidation can proceed through route 2 on Au/Ti-O.

4. Conclusions

In summary, this work demonstrates the roles of top Au sites on Au/

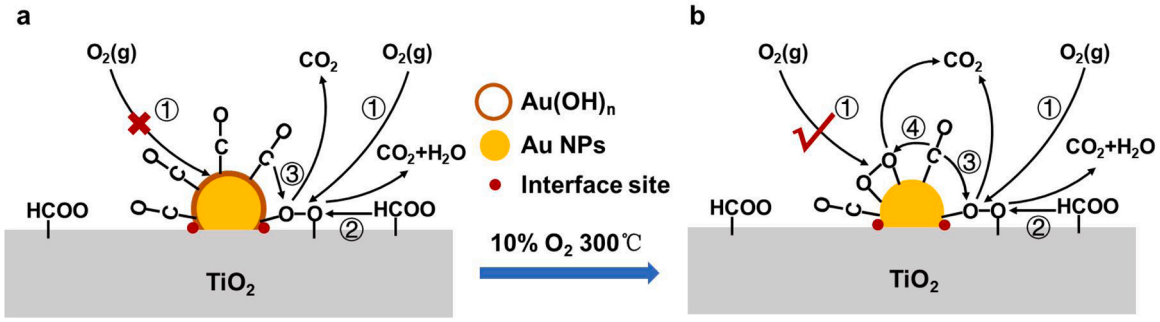

Fig. 7. Schematic illustration of the possible reaction mechanisms occurring on Au/Ti-F (a) and Au/Ti-O (b). Process 1: O_2 is activated at the Au-Ti interface or at top Au sites; process 2: HCOO reacts with adsorbed O at the interface; process 3: CO reacts with adsorbed O at the interface without HCHO; process 4: CO reacts with adsorbed O at top Au sites.

TiO_2 catalysts in HCHO and CO co-oxidation. It was found that both Au/Ti-F and Au/Ti-O show high activity in HCHO oxidation and CO oxidation reactions separately. However, Au/Ti-F shows high activity for HCHO oxidation but no activity for CO oxidation during HCHO and CO co-oxidation, while Au/Ti-O shows high activity for both HCHO and CO oxidation. We confirmed that the top Au sites and Au-Ti interface sites are both active sites on Au/Ti-O, on which HCHO oxidation occurs at the Au-Ti interface and CO oxidation can occur at the top Au sites, hence realizing high performance for HCHO and CO co-oxidation at room temperature. More importantly, we showed that the top Au sites are more active for CO oxidation than the Au-Ti interface sites. These findings on the multiple active sites on Au/TiO_2 provide new insight into the nature of the structures of the active sites on supported Au catalysts.

Supporting Information

Corresponding additional data: catalytic performance, in situ DRIFTS study, catalyst characterization results, DFT calculation results, and evaluation of activation energy.

CRediT authorship contribution statement

Xiaoxiao Qin: Investigation, Visualization, Methodology, Data curation, Formal analysis, Writing – original draft, Writing – review & editing; **Min Chen:** Conceptualization, Methodology, Formal analysis, Supervision, Writing – original draft, Writing – review & editing; **Xueyan Chen:** Formal analysis, the supporting of contribution; **Jianghao Zhang:** Formal analysis, the supporting of contribution; **Xiaoxin Wang:** Formal analysis, the supporting of contribution; **Jinhou Fang:** Resources, the supporting of contribution; **Hong He:** Resources, Supervision; **Changbin Zhang:** Conceptualization, Formal analysis, Resources, Supervision, Funding acquisition, Writing – review & editing.

Declaration of Competing Interest

The authors declare that they have no known competing financial interests or personal relationships that could have appeared to influence the work reported in this paper.

Data Availability

Data will be made available on request.

Acknowledgment

This work was financially supported by the National Natural Science Foundation of China (22025604, 21976196, 21936005, 22106171, 22276204).

Appendix A. Supporting information

Supplementary data associated with this article can be found in the online version at doi:10.1016/j.apcatb.2023.122663.

References

[1] C. Yu, D. Crump, A review of the emission of VOCs from polymeric materials used in buildings, Build. Environ. 33 (1998) 357–374.
[2] Y. Bruinen de Bruin, P. Carrer, M. Jantunen, O. Hanninen, G.S. Di Marco, S. Kephalopoulos, D. Cavallo, M. Maroni, Personal carbon monoxide exposure levels: contribution of local sources to exposures and microenvironment concentrations in Milan, J. Expo. Anal. Environ. Epidemiol. 14 (2004) 312–322.
[3] X. Hong, Deactivation of Pt-Au/TiO_2-CeO_2 catalyst for co-oxidation of HCHO, H_2 and CO at room temperature: degradations of active sites and mutual influence between reactants, Appl. Catal. A 582 (2019), 117116.
[4] J. Quiroz Torres, S. Royer, J.P. Bellat, J.M. Giraudon, J.F. Lamonier, Formaldehyde: catalytic oxidation as a promising soft way of elimination, ChemSusChem 6 (2013) 578–592.
[5] M. Haruta, T. Kobayashi, H. Sano, N. Yamada, Novel gold catalysts for the oxidation of carbon monoxide at a temperature far below 0℃, Chem. Lett. 16 (1987) 405–408.
[6] C. Zhang, H. He, A comparative study of TiO_2 supported noble metal catalysts for the oxidation of formaldehyde at room temperature, Catal. Today 126 (2007) 345–350.
[7] C. Zhang, F. Liu, Y. Zhai, H. Ariga, N. Yi, Y. Liu, K. Asakura, M. Flytzani-Stephanopoulos, H. He, Alkali-metal-promoted Pt/TiO_2 opens a more efficient pathway to formaldehyde oxidation at ambient temperatures, Angew. Chem. Int. Ed. 51 (2012) 9628–9632.
[8] Y. Li, C. Zhang, H. He, J. Zhang, M. Chen, Influence of alkali metals on Pd/TiO_2 catalysts for catalytic oxidation of formaldehyde at room temperature, Catal. Sci. Technol. 6 (2016) 2289–2295.
[9] Y. Li, C. Zhang, J. Ma, M. Chen, H. Deng, H. He, High temperature reduction dramatically promotes Pd/TiO_2 catalyst for ambient formaldehyde oxidation, Appl. Catal. B 217 (2017) 560–569.
[10] M. Haruta, S. Tsubota, T. Kobayashi, H. Kagyama, M.J. Genet, B. Delmon, Low-temperature oxidation of co over gold supported on TiO_2, α-Fe_2O_3, and Co_3O_4, J. Catal. 144 (1993) 175–192.
[11] M. Haruta, N. Yamada, T. Kobayashi, S. Iijima, Gold catalysts prepared by coprecipitation for low-temperature oxidation of hydrogen and of carbon monoxide, J. Catal. 115 (1989) 301–309.
[12] X. Zheng, J. Mantzaras, R. Bombach, Kinetic interactions between hydrogen and carbon monoxide oxidation over platinum, Combust. Flame 161 (2014) 332–346.
[13] S. Salomons, R.E. Hayes, M. Votsmeier, The promotion of carbon monoxide oxidation by hydrogen on supported platinum catalyst, Appl. Catal. A 352 (2009) 27–34.
[14] V. Muravev, G. Spezzati, Y.Q. Su, A. Parastaev, F.K. Chiang, A. Longo, C. Escudero, N. Kosinov, E.J.M. Hensen, Interface dynamics of Pd-CeO_2 single-atom catalysts during CO oxidation, Nat. Catal. 4 (2021) 469–478.
[15] W. Tan, S. Xie, Y. Cai, M. Wang, S. Yu, K.B. Low, Y. Li, L. Ma, S.N. Ehrlich, F. Gao, L. Dong, F. Liu, Transformation of highly stable Pt single sites on defect engineered ceria into robust Pt clusters for vehicle emission control, Environ. Sci. Technol. 55 (2021) 12607–12618.
[16] G. Spezzati, Y. Su, J.P. Hofmann, A.D. Benavidez, A.T. DeLaRiva, J. McCabe, A. K. Datye, E.J.M. Hensen, Atomically dispersed Pd-O species on CeO_2(111) as highly active sites for low-temperature CO oxidation, ACS Catal. 7 (2017) 6887–6891.
[17] B. Chen, C. Shi, M. Crocker, Y. Wang, A. Zhu, Catalytic removal of formaldehyde at room temperature over supported gold catalysts, Appl. Catal. B 132 (2013) 245–255.
[18] M. Haruta, T. Kobayashi, H. Sano, N. Yamada, Novel gold catalysts for the oxidation of carbon monoxide at a temperature far below 0℃, Chem. Lett. 16 (1987) 405–408.

[19] M. Haruta, N. Yamada, T. Kobayashi, S. Iijima, Gold catalysts prepared by coprecipitation xidation for low-temperature of hydrogen and of carbon monoxide, J. Catal. 115 (1988) 301–309.
[20] M. Haruta, Catalysis of gold nanoparticles deposited on metal oxides, Cattech 6 (2002) 102–115.
[21] H. Yoshida, Y. Kuwauchi, J.R. Jinschek, K. Sun, S. Tanaka, M. Kohyama, S. Shimada, M. Haruta, S. Takeda, Visualizing gas molecules interacting with supported nanoparticulate catalysts at reaction conditions, Science 335 (2012) 317–319.
[22] J. Saavedra, C.J. Pursell, B.D. Chandler, CO oxidation kinetics over Au/TiO_2 and Au/Al_2O_3 catalysts: evidence for a common water-assisted mechanism, J. Am. Chem. Soc. 140 (2018) 3712–3723.
[23] M. Haruta, Spiers memorial lecture. Role of perimeter interfaces in catalysis by gold nanoparticles, Faraday Discuss. 152 (2011) 11–32.
[24] F. Boccuzzi, A. Chiorino, M. Manzoli, P. Lu, T. Akita, S. Ichikawa, M. Haruta, Au/TiO_2 nanosized samples: a catalytic, TEM, and FTIR study of the effect of calcination temperature on the CO oxidation, J. Catal. 202 (2001) 256–267.
[25] Y. Zhang, J.X. Liu, K. Qian, A. Jia, D. Li, L. Shi, J. Hu, J. Zhu, W. Huang, Structure-sensitivity of Au-TiO_2 strong metal-support, Interact., Angew. Chem. Int. Ed. 60 (2021) 12074–12081.
[26] Z. Liu, X.Q. Gong, J. Kohanoff, C. Sanchez, P. Hu, Catalytic role of metal oxides in gold-based catalysts: a first principles study of CO oxidation on TiO_2 supported Au, Phys. Rev. Lett. 91 (2003), 266102.
[27] X. Chen, G. He, Y. Li, M. Chen, X. Qin, C. Zhang, H. He, Identification of a facile pathway for dioxymethylene conversion to formate catalyzed by surface hydroxyl on TiO_2-based catalyst, ACS Catal. 10 (2020) 9706–9715.
[28] C. Zhang, H. He, L. Wang, F. Jiang, H. Xing, O. Zhao, W. Bao, Review of noble metal catalysts for the oxidation of formaldehyde and air purification in indoor environment at room temperature, Chin. Sci. Bull. 54 (2009) 278–286.
[29] C.K. Costello, M.C. Kung, H.S. Oh, Y. Wang, H.H. Kung, Nature of the active site for CO oxidation on highly active Au/γ-Al_2O_3, Appl. Catal. A 232 (2002) 159–168.
[30] C.K. Costello, J.H. Yang, H.Y. Law, Y. Wang, J.N. Lin, L.D. Marks, M.C. Kung, H. H. Kung, On the potential role of hydroxyl groups in CO oxidation over Au/Al_2O_3, Appl. Catal. A 243 (2003) 15–24.
[31] H.S. Oh, C.K. Costello, C. Cheung, H.H. Kung, M.C. Kung, Regeneration of Au/γ-Al_2O_3 deactivated by CO oxidation, Stud. Surf. Sci. Catal. 139 (2001) 375–381.
[32] G.C. Bond, D.T. Thompson, Gold-catalysed oxidation of carbon monoxide, Gold. Bull. 33 (2000) 41–50.
[33] I.X. Green, W. Tang, J.T.Y. M. Neurock Jr., Spectroscopic observation of dual catalytic sites during oxidation of CO on a Au/TiO_2 catalyst, Science 333 (2011) 736–739.
[34] T. Fujitani, I. Nakamura, Mechanism and active sites of the oxidation of CO over Au/TiO_2, Angew. Chem. Int. Ed. 50 (2011) 10144–10147.
[35] L.B. Vilhelmsen, B. Hammer, Identification of the catalytic site at the interface perimeter of Au clusters on rutile TiO_2(110), ACS Catal. 4 (2014) 1626–1631.
[36] W. Yuan, B. Zhu, K. Fang, X.Y. Li, T.W. Hansen, Y. Ou, H. Yang, J.B. Wagner, Y. Gao, Y. Wang, Z. Zhang, In situ manipulation of the active Au-TiO_2 interface with atomic precision during CO oxidation, Science 371 (2021) 517–521.
[37] I.N. Remediakis, N. Lopez, J.K. Norskov, CO oxidation on rutile-supported Au nanoparticles, Angew. Chem. Int. Ed. 44 (2005) 1824–1826.
[38] M. Valden, X. Lai, D.W. Goodman, Onset of catalytic activity of gold clusters on titania with the appearance of nonmetallic properties, Science 281 (1998) 1647–1650.
[39] M. Chen, D.W. Goodman, Catalytically active gold: from nanoparticles to ultrathin films, Acc. Chem. Res. 39 (2006) 739–746.
[40] Y. Kuwauchi, H. Yoshida, T. Akita, M. Haruta, S. Takeda, Intrinsic catalytic structure of gold nanoparticles supported on TiO_2, Angew. Chem. Int. Ed. 51 (2012) 7729–7733.
[41] R. Si, M. Flytzani-Stephanopoulos, Shape and crystal-plane effects of nanoscale ceria on the activity of Au-CeO_2 catalysts for the water-gas shift reaction, Angew. Chem. Int. Ed. 47 (2008) 2884–2887.
[42] J. Zhang, L. Di, F. Yu, D. Duan, X. Zhang, Atmospheric-pressure cold plasma activating Au/P25 for CO oxidation: effect of working gas, Nanomater. (Basel) 8 (2018) 742.
[43] F. Moreau, G. Bond, A. Taylor, Gold on titania catalysts for the oxidation of carbon monoxide: control of pH during preparation with various gold contents, J. Catal. 231 (2005) 105–114.
[44] L. Wang, Y. Zhong, D. Widmann, J. Weissmüller, R.J. Behm, Oxygen adsorption and low-temperature CO oxidation on a nanoporous Au catalyst: reaction mechanism and foreign metal effects, Top. Catal. 61 (2018) 446–461.
[45] S. Chenakin, N. Kruse, Combining XPS and ToF-SIMS for assessing the CO oxidation activity of Au/TiO_2 catalysts, J. Catal. 358 (2018) 224–236.
[46] X. Qin, M. Chen, X. Chen, J. Zhang, X. Wang, J. Fang, C. Zhang, Effects of the metal–support interaction in Ru/CeO_2 nanostructures on active oxygen species for HCHO/CO oxidation, ACS Appl. Nano Mater. 5 (2022) 15574–15582.
[47] J. Huang, S. He, J.L. Goodsell, J.R. Mulcahy, W. Guo, A. Angerhofer, W.D. Wei, Manipulating atomic structures at the Au/TiO_2 interface for O_2 activation, J. Am. Chem. Soc. 142 (2020) 6456–6460.
[48] W. Grunert, D. Grossmann, H. Noei, M.M. Pohl, I. Sinev, A. De Toni, Y. Wang, M. Muhler, Low-temperature oxidation of carbon monoxide with gold(III) ions supported on titanium oxide, Angew. Chem. Int. Ed. 53 (2014) 3245–3249.
[49] Z. Duan, G. Henkelman, Calculations of CO oxidation over a Au/TiO_2 catalyst: a study of active sites, catalyst deactivation, and moisture effects, ACS Catal. 8 (2018) 1376–1383.
[50] S. Wei, W.W. Wang, X.P. Fu, S.Q. Li, C.J. Jia, The effect of reactants adsorption and products desorption for Au/TiO_2 in catalyzing CO oxidation, J. Catal. 376 (2019) 134–145.
[51] H. Tang, Y. Su, B. Zhang, A.F. Lee, M.A. Isaacs, K. Wilson, L. Li, Y. Ren, J. Huang, M. Haruta, B. Qiao, X. Liu, C. Jin, D. Su, J.H. Wang, T. Zhang, Classical strong metal-support interactions between gold nanoparticles and titanium dioxide, Sci. Adv. 3 (2017), e170023.
[52] S. Wei, X. Fu, W. Wang, Z. Jin, Q. Song, C. Jia, Au/TiO_2 catalysts for CO oxidation: effect of gold state to reactivity, J. Phys. Chem. C. 122 (2018) 4928–4936.
[53] P. Perez, M.A. Soria, S.A.C. Carabineiro, F.J. Maldonado-Hodar, A. Mendes, L. M. Madeira, Application of Au/TiO_2 catalysts in the low-temperature water-gas shift reaction, Int. J. Hydrog. Energ. 41 (2016) 4670–4681.
[54] J. Saavedra, H.A. Doan, C.J. Pursell, L.C. Grabow, B.D. Chandler, The critical role of water at the goldtitania interface in catalytic CO oxidation, Science 345 (2014) 1599–1602.